

EXPERIMENTAL CHARACTERIZATION OF ACOUSTIC PRESSURE WAVES PROPAGATING IN CIRCULAR DUCTS

Giovanni Ferrara¹, Lorenzo Ferrari^{2*}, Giulio Lenzi¹

¹) "Sergio Stecco" Department of Energy Engineering, University of Florence
Via S. Marta 3, 50139, Firenze (FI), Italy

²) ICCOM CNR, National Research Council of Italy
Via Madonna del Piano 10, 50019, Sesto Fiorentino (FI), Italy

*) Contact Author: Ph. +39 055 4796 570 - Fax +39 055 4796 342; e-mail: ferrari@iccom.cnr.it

ABSTRACT

The increasing interest in thermoacoustic phenomena in turbomachinery components prompted a detailed analysis of acoustic field propagation in ducts. The numerical codes for the prediction of the acoustic behavior of complex system are still in a developing phase and an experimental validation is still necessary. The wall acoustic pressure could be easily measured whereas very few examples of radial measurement, necessary for a 3D analysis, are present in the literature. In this paper, several simple remote probes mounting a 1/4" pressure microphone are characterized. The one, performed best, is used to map the acoustic pressure field of a wave propagating in a circular duct with different modes. The experimental set up and the calculation methodology are shown in detail in the paper.

INTRODUCTION

New generation combustors, based on a lean combustion technology, are very sensitive to thermoacoustic phenomena. For this reason the analysis of acoustic pressure wave propagation and interaction with boundary walls are gaining increasing interest. Since the behavior of an acoustic pressure wave is strongly dependent on its mode, many experimental activities are now focused on the characterization of wave pressure distribution during its propagation in ducts [1, 2]. In turbomachinery applications, for example, many investigations are carried out on the interaction between the combustion chamber liner (acting as acoustic dumping device) and the thermo-acoustic instability of the flame [3]. The typical approach is limited to the analysis of the wall pressure distribution by means of flush mounted microphones. This methodology allows the measurement of the planar and tangential distribution only and does not give any information on the radial pressure trend. This lack of data makes a 3D reconstruction of the acoustic pressure wave difficult. Only few limited examples of indirect estimation of pressure distribution can be found in the literature. These are based on the acoustic velocity estimation by PIV [4] and LDV [5] measurement techniques. Another solution, much simpler to set up, could be the adoption of a wave guide probe. This is generally made up of a transmitting duct and a sensor housing placed at one of its ends. This system would allow the direct estimation of the acoustic pressure values along the span even in presence of hot flow. The main issue limiting the wave guide probe application is the high number of peaks and valleys of their frequency response function. This trend is due to the duct resonances and the reflected wave generated by the variation of diameter between the duct and the measurement chamber. The adoption of a long dumping duct behind the sensor (about 30 m) [6] or a dissipating chamber ([7] and [8]) are typical solutions to these problems. The common applications of these systems are the dynamic pressure measurement in turbomachinery components ([9] and [10]). For the radial acoustic pressure measurement, the probe has to be much smaller than the duct diameter and then also smaller than the microphone diameter (typically 1/4" in order to have high sensitivity). Therefore the adoption of a dumping element would not solve the presence of a reflected wave since a chamber for the microphone housing is inevitably present.

Within this context, several wave guide probes, with different geometries and housing a 1/4" microphone, are designed and tested to identify which solution has the best frequency response function. The range of interest is limited to a frequency below 5 kHz in order to investigate the first radial mode. The probe with the best frequency response function is used to estimate the acoustic pressure map in three different propagating conditions in a straight circular duct. The pressure maps are estimated measuring the acoustic pressure in twelve circumferential and nine radial positions. The experimental procedure, the numerical analysis and an estimation of the error related to the measurement approach (e.g. the probe tip positioning) are discussed in this paper.

ACOUSTIC WAVE FIELD PROPAGATION IN CIRCULAR DUCTS

The propagation of a sound wave field in a circular infinite duct is described by the convective wave equation that for a hard wall duct is expressed as in Eq. 1.

$$\left(\frac{D^2}{Dt^2} - c^2 \nabla^2 \right) p(x, \theta, r, t) = 0 \tag{Eq. 1}$$

The solution of Eq. 1 by the variables separation method in a cylindrical duct with radius R without mean flow, gives the acoustic pressure distribution along the duct (Eq. 2) for a given acoustic pressure source (p_{mf}). The acoustic pressure distribution turns out to be the sum of several acoustic modes (indicated with a m and n index pairs). Index m describes the circumferential pressure distribution, typically sinusoidal. Index n indicates the radial pressure distribution. This follows a first order Bessel function whose argument κ_{mn} is related to the pressure gradient calculated on the duct wall (Fig. 1). In the axial direction, each mode decays independently with an exponential law with coefficient Γ .

$$p(\theta, r, x, t) = \sum_{m=0}^M \sum_{n=0}^N p_{mf} J_m(\kappa_{mn} r) \times \exp[i\Gamma x + im\theta + i\omega t] \tag{Eq. 2}$$

$$\Gamma^\pm = \mp \sqrt{\frac{\kappa_{mn}^2}{\eta^2} - 1}$$

The coefficient κ_{mn} is also involved in the calculation of the axial decay coefficient Γ which determines if the acoustic mode propagates through the duct or not. If the axial index (Γ) is real, the acoustic mode propagates otherwise, if it is imaginary, the acoustic field decays. The frequencies for which a mode starts to propagate are named cut-on frequencies; on the contrary the ones for which a mode decays are named cut-off frequency. For the $m=0$ mode, the cut on frequency is 0Hz.

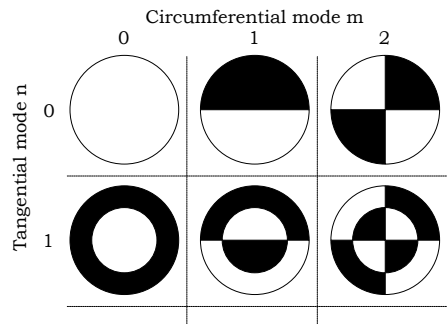


Fig. 1 Schematic shapes of acoustic modes

If one considers a 150 mm diameter duct, the cut on and off frequencies of an acoustic wave are reported in Table 1. The total acoustic wave field for a given frequency is the superposition of the propagating modes. For example, in a frequencies range between 1.39 and 2.28 kHz both planar wave field ($m=0, n=0$) and first mode ($m=1, n=0$) propagate: the total acoustic field is given by the complex sum of the two modes.

		m					
		0	1	2	3	4	5
n	0	2892 Hz	1390 Hz	2280 Hz	3171 Hz	3949 Hz	4784 Hz
	1	5229 Hz	4005 Hz	5006 Hz	5952 Hz	6898 Hz	7844 Hz

Table 1. Cut-on and cut-off frequencies for a 150 mm diameter duct.

When the frequency increases the acoustic wave field becomes more and more complex; if one considers a frequency range between 3.95 and 4.78 kHz, the acoustic pressure field turns out to be made up of three modes: the fourth tangential ($m=4, n=0$ Fig. 2-a), the zero radial ($m=0, n=1$ Fig. 2-b) and first radial ($m=1, n=1$ Fig. 2-c) modes.

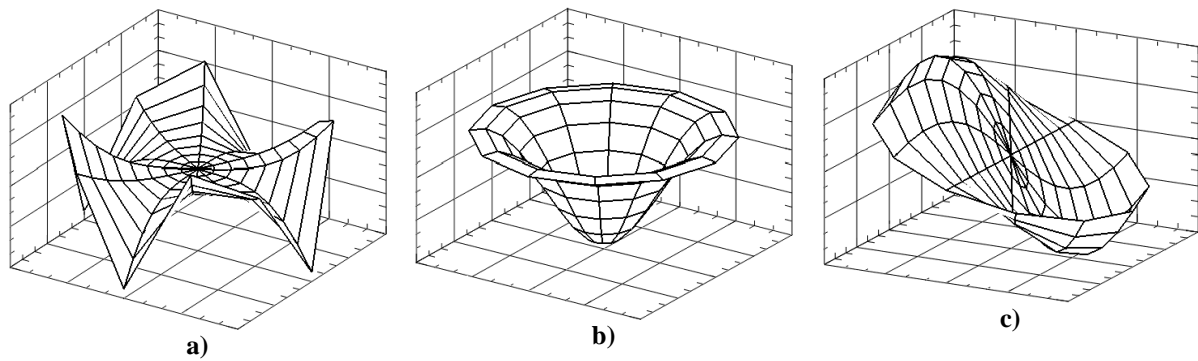


Fig. 2. Theoretical single modes at 4.1 kHz

In case of a semi-infinite duct, with an acoustic source at one end, only one travelling wave with characteristics described before propagates. In case of a finite length duct or in presence of discontinuities, the global pressure field is made up of two travelling waves that propagates in opposite direction: the one from the acoustic source (incident wave) and that reflected by the discontinuity (reflected wave). Along the duct, the superposition of the two travelling wave fields is a standing wave. In a generic section of the duct, the combination of the incident and reflected waves generates an oscillating field, instead of a rotating one, with the distribution of the incident wave.

EXPERIMENTAL SET UP

The experimental activity (acoustic wave field mapping and probe calibration) is performed on a circular duct of Silere which is an acoustic dumping material. On one hand, the acoustic source is made up of four compressor drivers (Monacor® KU616T), mounted in radial direction and equally spaced; on the other hand the duct is open to air. The source signal is generated by a waveform generator (Agilent® 33220A) and amplified with a power amplifier (Monacor® PA-940). The duct has a diameter of 150 mm and a total length of 6 m. The measurement section is placed at five diameters from acoustic source, the rest of the duct is used to dump both incident and reflected waves to make the acoustic field in the measurement section as close as possible to the one of semi-infinite condition (Fig. 3). Twelve microphones are used to measure the tangential acoustic wave field. They are flush mounted and equally spaced in the circumferential direction. A microphone placed 60 mm upstream the measurement section is used as a reference to clock the signals in different measurement sessions. The radial acoustic pressure measurement for different angular positions is performed replacing one of the twelve microphones with the wave guide probe. All the acoustic pressure measurements are carried out with G.R.A.S.® 1/4" pressure type microphone. The acquisition software is developed in Labview® and the signals are acquired by a National Instruments® device with a maximum sampling rate of 51,2 kSamples/.

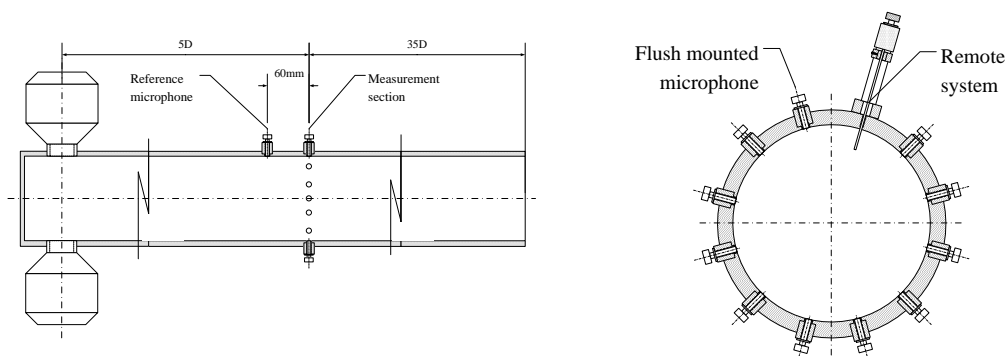


Fig. 3. Scheme of test rig for probe characterization and wave field mapping

REMOTE PROBE DESIGN AND CALIBRATION

The measurement of wave fields with tangential distribution is commonly performed with flush mounted microphones placed on the duct wall. To perform a radial pressure measurement it is necessary to estimate the acoustic pressure at different radii without interference with the field itself. For this reason it is generally used a probe instead of a local direct measurement. A typical probe for this application is reported in Fig. 3. This device is made up of a transmitting duct and a sensor housing placed at one of its ends.

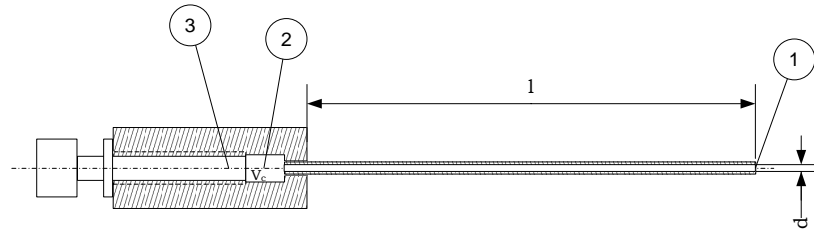


Fig. 3. Scheme of remote probe; 1) Transmission duct; 2) Chamber; 3) Microphone 1/4"

The main issue limiting the application of this kind of probes is their frequency response that is characterized by several peaks and valleys. Such distortion are due to the transmitting duct resonances and to the reflected wave generated by the variation of diameter between the duct and the measurement chamber. Therefore, the geometry of the connection between the transmitting duct and the chamber, the microphone dimension and the cavity of sensor housing play a key role.

In order to choose a probe geometry that could minimize the frequency distortion, an extended experimental campaign is performed. A transmission duct with a diameter of 2 mm and 120 mm long is considered. The housing chamber is 10 mm long and, due to the microphone dimensions, has a diameter of 8 mm. The probe geometries investigated are (Fig. 4):

- 1) Case A: back mounted microphone with abrupt connection (baseline)
- 2) Case B: flush mounted microphone with abrupt connection
- 3) Case C: back mounted microphone with conical connection
- 4) Case D: flush mounted microphone with conical connection
- 5) Case E: flush mounted microphone with conical connection and extended chamber (30 mm)
- 6) Case F: flush mounted microphone with conical connection and damping duct of 30 m

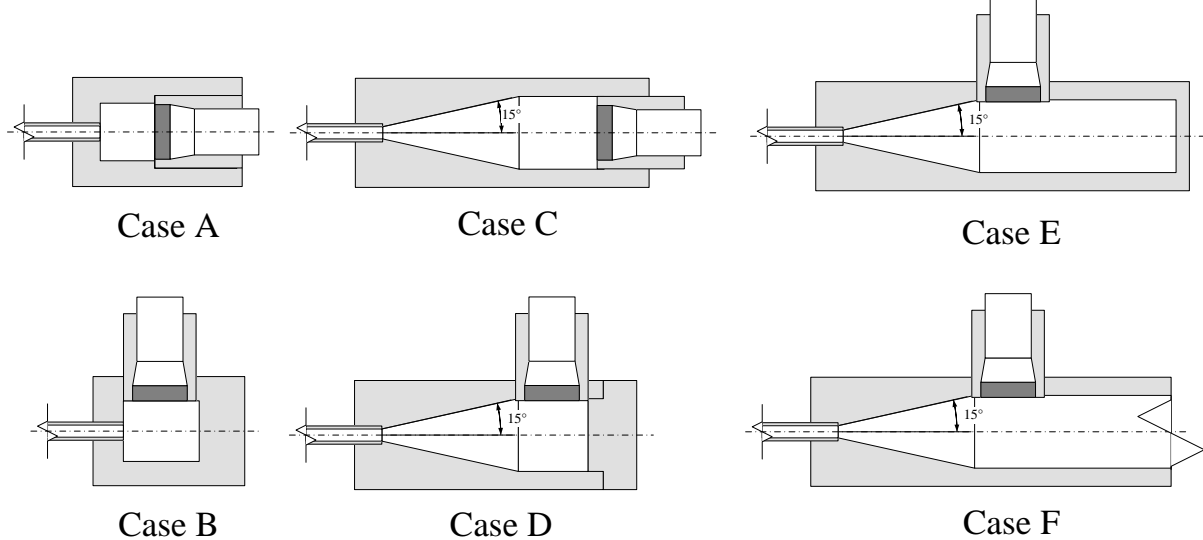


Fig. 4. Schemes of the probes realized

The comparisons between the probes are performed with a planar wave field (up 1.3 kHz) because this distribution is characterized by an equal amplitude and phase in every point of the measurement section. For greater frequencies the presence of additional modes would have made the calibration procedure too complex for the comparison purposes. The probe is moved back so that the transmission duct end is aligned with the inner duct wall. The acoustic pressure measured by the microphone is compared with the one of a flush mounted microphone in the same section. Microphone signals are acquired for 1 second and analyzed with a FFT approach. The main results are reported in Fig. 5 to Fig. 8 in terms of Frequency Response Function (FRF), Eq. 3. This is the ratio between the pressure measured by the reference microphone on the one measured by the probe both considered as complex quantities and then having a modulus and a phase.

$$FRF = \frac{\hat{p}_{mic}}{\hat{p}_{probe}} \quad \text{Eq. 3}$$

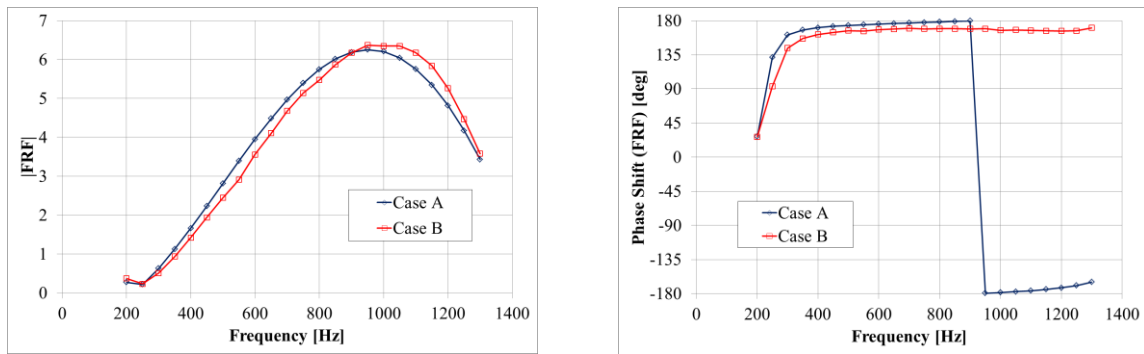


Fig. 5. Comparison of frequency response function for Case A and B

The comparison of the plots in Fig. 5 (Case A and B) shows that the position of the microphone does not deeply affect the frequency response of the probe. The difference in frequency response due to the sensor position increases when a conical connection is considered (Case C and D, Fig. 6).

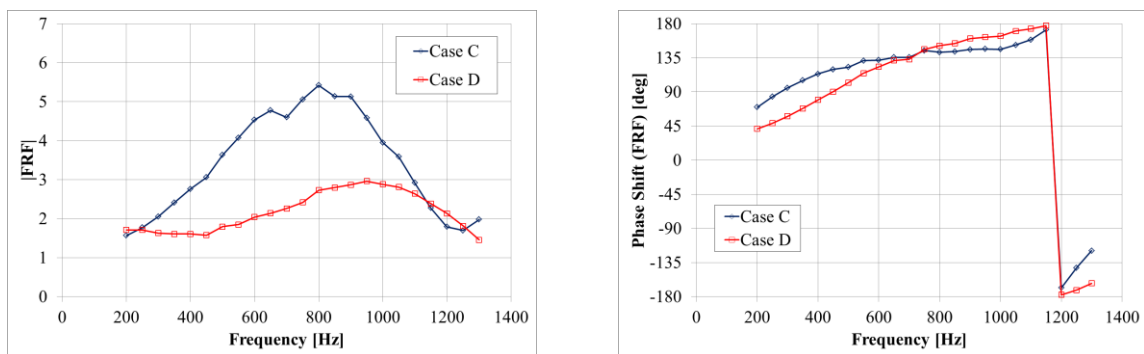


Fig. 6. Comparison of frequency response function for Case C and D

As a general trend, the conical connection reduces the pressure losses in the transition between the transmission duct and the housing chamber. In particular the best results are achieved with the flush mounted configuration.

A common practice to reduce the detrimental effects of the transmission duct resonance is the use of a damping duct several meters long placed at the end of the housing chamber [1]. The influence of a 30 m long damping duct and of an extended housing chamber dimension are reported in Fig. 7 (Case D, E and F). As expected, the increasing of the chamber dimension has a detrimental effect on the probe FRF. An unexpected result is the worsening of the FRF in case of a dumping duct. This result confirms the relevance of the housing chamber dimension on the probe FRF.

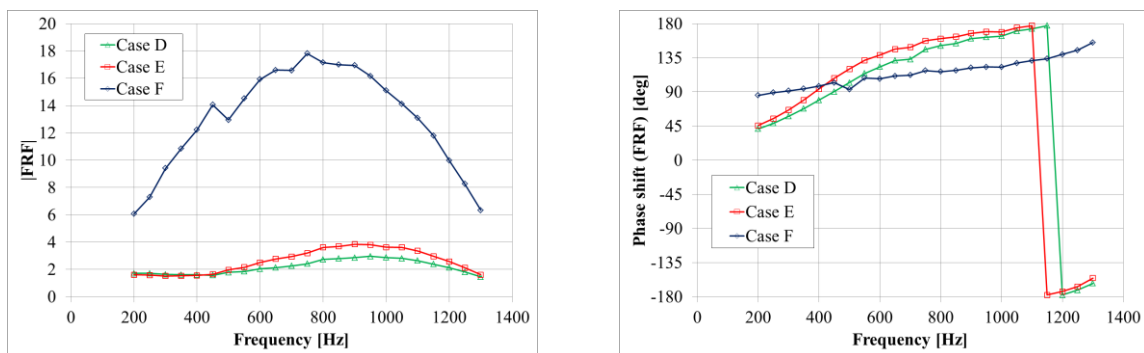


Fig. 7. Comparison of frequency response function for Case D, E and F.

From the comparison of all the results, the probe with a conical connection, a small housing chamber and a flush mounted microphone has the best FRF. For that probe, the experimental calibration is extended up to 4.5 kHz (as depicted in Fig. 8) because the dependence of acoustic pressure on radial position starts, for the described test rig, from 4.0 kHz.

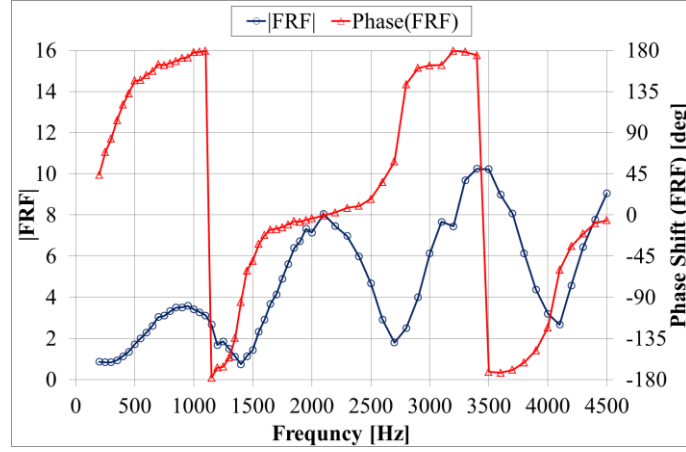


Fig. 8. Extended characterization

For frequencies higher than the first cut-on frequency, the acoustic pressure on the duct wall is no more uniform but changes with the position (x', r, θ) . To estimate the FRF of the probe at high frequency, the measurement of acoustic pressure at wall radius has to be made in two times (1 and 2) in the same measurement position (x', R, θ) . In the first session the acoustic pressure field is measured by the reference microphone (*ref*) and the probe. In the second session the same condition of session 1 on the reference microphone is reproduced and the probe is replaced by a flush mounted microphone. The FRF is therefore calculated as the ration between the second and the first measurement (Eq. 4).

$$FRF = \frac{\hat{p}_{mic}^{(1)}(x', R, \theta)_{ref(1)}}{\hat{p}_{probe}^{(2)}(x', R, \theta)_{ref(2)}} \quad \text{Eq. 4}$$

ACOUSTIC FIELD MAPPING

Data analysis methods

The acoustic pressure distribution in the duct cross section is the result of two waves moving in opposite directions. In each measurement point the pressure field is characterized by an amplitude and a phase, the two parameters depending on the geometrical set up of the test rig (distance from the acoustic the source, the sound pressure level of the source, measurement section and duct termination).

The description of acoustic wave fields needs several measurement points. In this activity the pressure distribution is measured by twelve measurement points in tangential direction and nine positions along twelve radii. As consequence, the wave field reconstruction involves twelve measurement sessions, where both the tangential distribution and the one along a radius are acquired. In addition to the previous ones, also the reference microphone signal is recorded. These data are used to clock the twelve measurement sessions and scale the amplitude (Eq. 5).

$$p_{map}(r, \theta) = \frac{|p_{r\theta}|}{|p_{ref}|} \cos(\varphi_{r\theta}|_{mic_{ref}}) \quad \text{Eq. 5}$$

Data fitting procedure

The pressure measurements are used to create a map of the acoustic field. Raw data are fitted with an interpolation procedure. The residuals of the fitting procedure need to be compared with the errors related to the measurement procedure and in particular they have to be lower than the errors due to the probe tip positioning. The position of the probe strongly affects the measurement of acoustic pressure. By making the hypothesis that pressure amplitude change is negligible for small axial variations, a wrong positioning of probe tip causes a shift in signal phase and consequently an error on the estimation of acoustic wave field pressure. The relevance of this error, that depends on the frequency, is estimated for different tip positioning and depicted in Fig. 9.

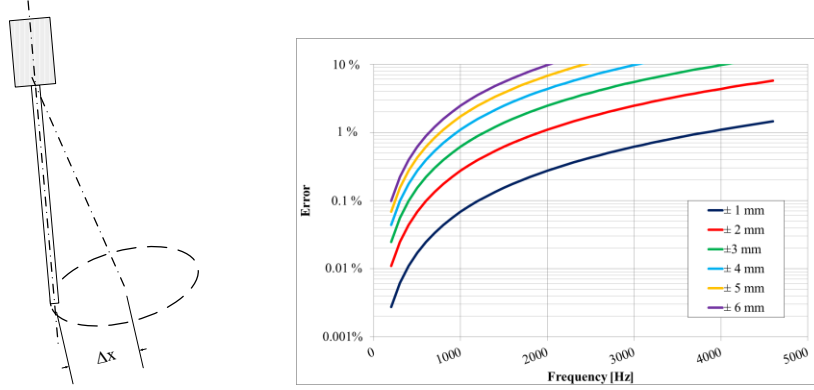


Fig. 9. Error on phase measurement due to uncertainties of tip probe placing

To estimate the placing error experimentally, the characteristics of the first tangential mode ($m=1, n=0$) is exploited. This mode has a linear pressure distribution along the radial span. Due to the presence of the planar wave field the linear distribution has a finite value in the middle of the duct (instead of a null value). This value can be calculated as the mean value between the maximum and minimum acoustic pressure measured by the flush mounted microphones in the measuring section (Eq. 6).

$$|p_{00}| = \frac{\max[|\hat{p}_\theta| \cos(\varphi_\theta)] + \min[|\hat{p}_\theta| \cos(\varphi_\theta)]}{2} \quad \text{Eq. 6}$$

If one subtracts the amplitude of planar wave field calculated by Eq. 6 from the acoustic pressure distribution in the duct, the first tangential mode distribution is obtained. This distribution has a null value in the middle of the duct at measurement section; if the probe measures a pressure different from zero for that span, probably a tip displacement error is present, this causing a δp . To estimate the tip displacement from the theoretical position is assumed the hypothesis that the variation in the axial direction of planar acoustic field amplitude between the theoretical and actual probe position can be neglected. Since a standing wave has a sinusoidal trend in the axial direction it is possible to calculate the phase difference corresponding to the pressures estimated in the measurement section at tip probe position. The phase difference can be related to the axial displacement by considering the wave length (Eq. 7).

$$\Delta \bar{x} = \arcsen\left(\frac{p(\theta)|_{r=0} - |p_{00}|}{|p_{00}|}\right) * \frac{c}{2\pi f} \quad \text{Eq. 7}$$

Since the wall positioning of the probe is geometrically verified and all the measurement points lay on the same plane, the displacement error can be estimated as a linear distribution along the radius (Eq. 8).

$$\Delta x(r) = r * \text{arctg}\left(\frac{\Delta \bar{x}}{r_{\text{duct}}}\right) \quad \text{Eq. 8}$$

The same procedure is carried out for all the twelve circumferential positions and the estimation of the radial measurement is carried out (Fig. 10). The pressure at the middle of the duct considered for the calculation of the distribution map is the one with the minimum displacement error among the twelve measurement.

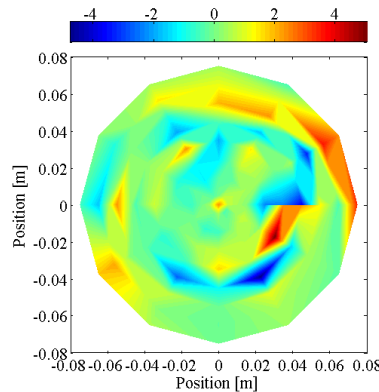


Fig. 10. Probe tip positioning error (%) estimated for Case D probe, flush mounted microphone with conical connection.

Experimental wave field mapping

The pressure distribution maps are measured for three propagating wave field of increasing complexity:

- 1) From 1.39 to 2.28 kHz , complex sum of planar mode ($m=0, n=0$) and first tangential mode ($m=1, n=0$);
- 2) From 2.28 to 3.17 kHz, complex sum of planar mode ($m=0, n=0$) and the second tangential mode ($m=2, n=0$);
- 3) From 3.95 to 4.78 kHz 4.1 kHz, complex sum of three modes, the fourth tangential ($m=4, n=0$), the zero radial ($m=0, n=1$) and first radial ($m=1, n=1$).

The frequencies for which the propagating fields are investigated are the ones where the frequency response function of the probe has a minimum. The measurement are carried out with both Case D and Case A probes with the aim of comparing the FRF influence on the results. The calibration coefficient for the two probes are reported in Table 2.

Field type	Case A			Case D		
	Frequency [kHz]	Gain	Phase Shift	Frequency [kHz]	Gain	Phase Shift
n. 1	1.8	4.29	-17°	1.5	1.40	-50°
n. 2	2.8	4.61	100°	2.7	1.79	58°
n. 3	4.1	3.49	-81°	4.1	2.66	-60°

Table 2. comparison of best calibration of the two probe in each propagation mode rage

All the pressure maps are referred to the reference microphone pressure and reported in Fig. 11 to Fig. 16. In order to compare the results, the data raw for the two probes (linear interpolation), the fitted values (lower cubic) for Case D probe and the theoretical distributions are reported for the three propagating fields. The theoretical maps considers both the incident and reflected wave in analogy with what is measured by the probes. For the theoretical distributions it is not possible to know the phase difference between the incident and reflected wave for non-planar modes since it is not possible to characterize the duct end behavior. In the Figures below the same phase shift is considered for the planar wave and all the other modes.

In Fig. 11 and Fig. 12, the pressure distribution for condition 1, are reported. The overall acoustic pressure distribution has a linear trend in the radial direction. The map measured with the Case D probe has a more uniform distribution than the one measured by the other. The fitted distribution turns out to be in good agreement with the theoretical one.

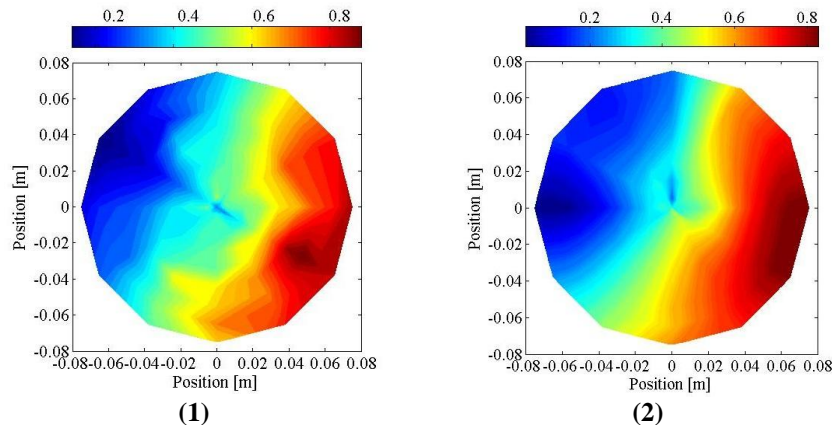


Fig. 11. Comparison of experimental maps of first tangential mode ($m=1, n=0$) measured with probe Case A, back mounted microphone with abrupt connection (1) and D, flush mounted microphone with conical connection (2)

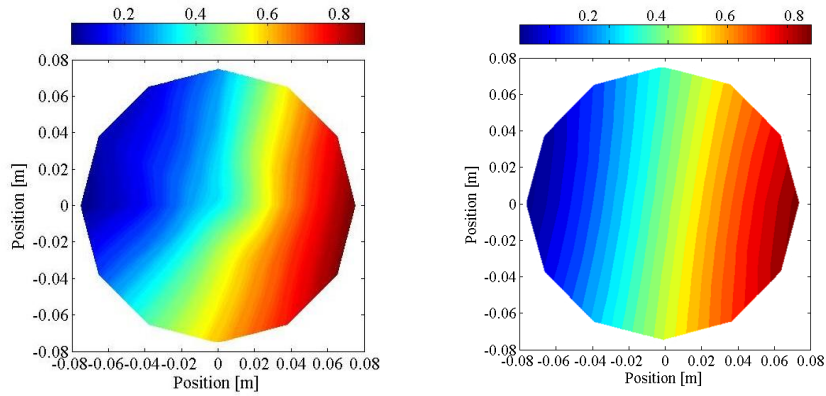


Fig. 12. Comparison of first tangential mode ($m=1, n=0$) with theoretical wave field

In Fig. 13 and Fig. 14, the pressure distribution for condition 2, are reported. The results are similar to those of the previous case. The distribution is not symmetrical as in theoretical distribution (Fig. 14), because the phase of the tangential second mode is not the same that in the theoretical map.

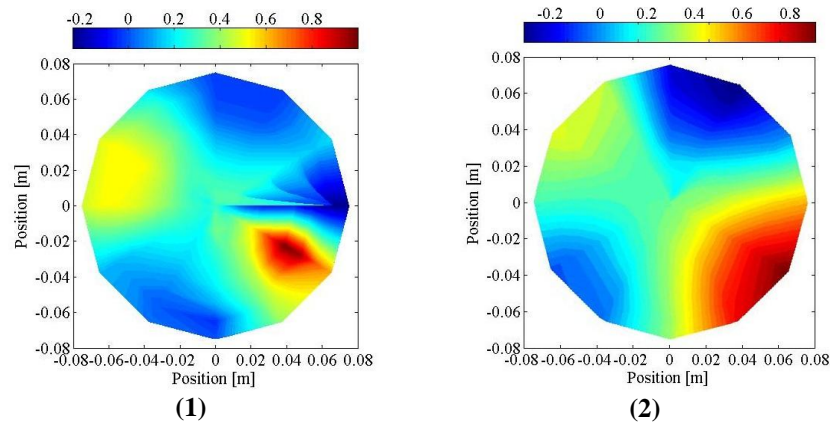


Fig. 13 Comparison of experimental maps of second tangential ($m=2, n=0$) mode measured with probe Case A, back mounted microphone with abrupt connection (1) and D, flush mounted microphone with conical connection (2)

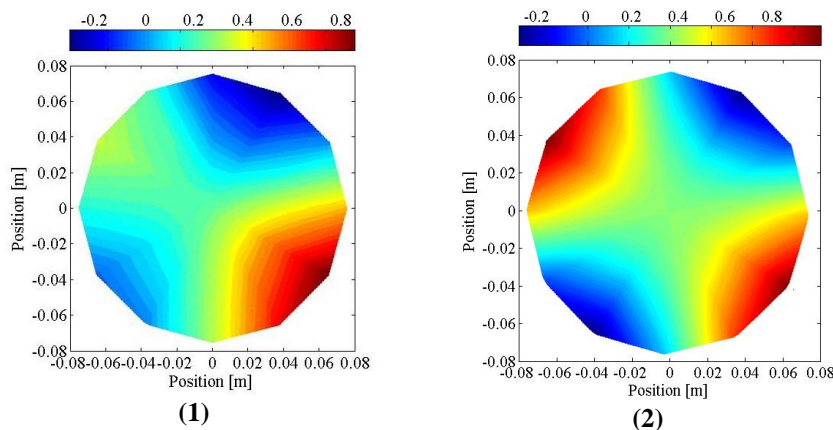


Fig. 14 Comparison of second tangential mode ($m=2, n=0$) with theoretical wave field

In Fig. 15 and Fig. 16, the pressure distribution for condition 3, are reported. Even for this test case probe Case D needs lesser gain and consequently has lesser error amplification. Also in this case a good agreement with the theoretical distribution is achieved.

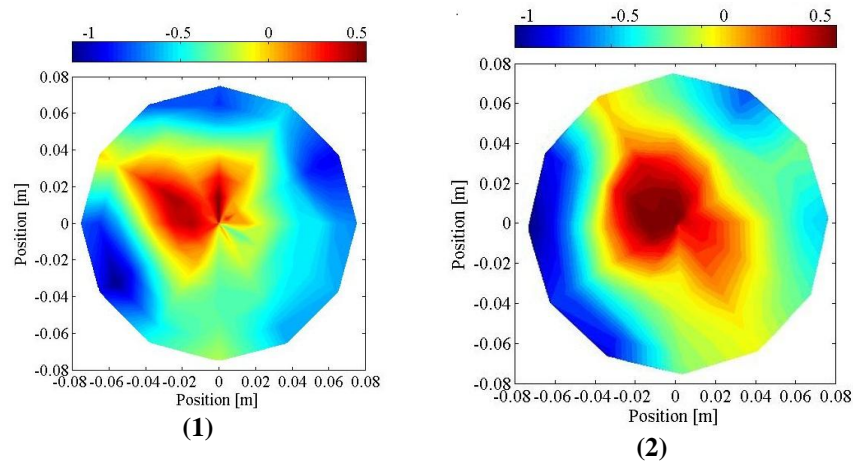


Fig. 15. Comparison of experimental maps at 4.1 kHz measured with probe Case A, back mounted microphone with abrupt connection (1) and B, flush mounted microphone with conical connection (2)

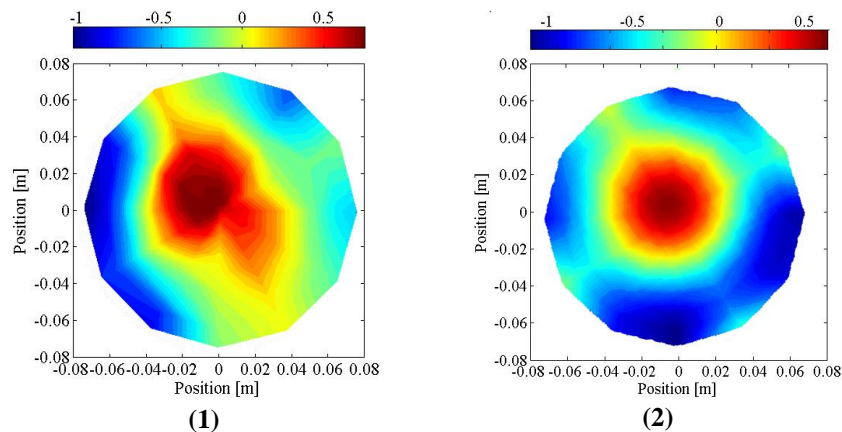


Fig. 16 Comparison of experimental maps at 4.1 kHz with theoretical map

CONCLUSION

In recent years, the analysis of acoustic wave propagation in ducts has become more and more important thanks to the relevant effects of acoustic perturbations on flame stability. Many numerical tools can be adopted for the investigation of acoustic wave propagation, whereas from the experimental point of view, only a few solutions are available, especially if a 2D characterization of the wave is sought. A common practice is the adoption of a wave guide probe, made-up of a transmitting duct and a housing chamber for a microphone. The larger the microphone diameter is the higher its sensitivity. On the other hand, larger diameters involve greater discontinuity between the transmission duct and the microphone housing and then more distorted frequency response functions. Several geometries of microphone housing have been investigated in this paper. Among them the one with a conical connection between the transmission duct and sensor housing and the microphone mounted orthogonally to the cone axis shows the best results. This probe is used for the measurement of the acoustic wave field propagating in a semi-infinite circular duct considering twelve circumferential positions and nine radial displacements. An procedure is developed for the estimation of the errors due to probe tip placing. The acoustic pressure map is experimentally reconstructed for three different propagating acoustic field with increasing complexity: the first and the second tangential modes characterized by the complex sum of planar wave field and the tangential one, and the acoustic field at 4.1kHz which is made up of three different field the forth tangential and the zero and first radial. Experimental data are compared with theoretical acoustic fields taking into account that the experimental map is made up of both incident and reflected waves. A good agreement is found between the experimental and the theoretical results.

The results achieved with this work demonstrate that with a properly calibrated probe it is possible to reconstruct also the radial acoustic pressure distribution of a propagating acoustic field. This is a quite new result in the field of acoustic pressure wave propagation analysis.

NOMENCLATURE

c	Sound velocity
FRF	Frequency response function
J	Bessel first order function
i	Time index
L	Duct length
m	Tangential mode index
n	Radial mode index
p_{mnf}	Acoustic pressure for mn mode
\hat{p}	Complex pressure
p_{mn}	Pressure evaluated for mode m,n
R	Radius of the duct
r	radial coordinate
x	Axial position
λ	Wave length
Γ	Axial decay coefficient
θ	Position on circumference
φ	Phase shift
κ_{mn}	Roots of square root of decay coefficient
$\eta = \frac{\omega r}{c}$	
ω	Angular frequency

ARKNOWLEDGMENTS

Thanks are due to Prof. Ennio Antonio Carnevale of the University of Florence for supporting this study.

REFERENCES

- [1] J. M. Verdon, M. D. Montgomery e K. A. Kousen, «Developmento of linearized unsteady Euler analysis for tubomachinery blade rows,» NASA, East Hartford, Connecticut, 1995.
- [2] D. L. Sutliff, «Rotating Rake Turbofan Duct Mode Measurement system,» NASA, Cleveland, Ohio, 2005.
- [3] A. Andreini, B. Facchini, L. Ferrari, G. Lenzi, F. Simonetti e A. Peschiulli, «Experimental investigation on effusion liner geometry for aero-engine combustors: evaluation of globa acoustic parameter,» Accepted for *ASME Turbo Expo 2012*, Copenhagen, Denmark, 2012.
- [4] A. Fischer, E. Sauvage e I. Röhle, «Acoustic PIV: Measurements of the acoustic particle velocity using synchronized PIV-technique,» in *14th Int Symp on Applications of Laser Techniques to Fluid Mechanics*, Lisbon, 2008.
- [5] G. Souchon, B. Gazengel, O. Richoux e A. L. Duff, «Characterization of a dipole radiation by Laser Doppler Velocimetry,» 2004.
- [6] G. Ferrara, L. Ferrari e G. Sonni, «Experimental characterization of a remoting system for dynamic pressure sensors,» in *ASME TURBO EXPO*, Reno-Tahoe, Nevada, USA, 2005.
- [7] H. Tijdeman, «Investigation of the transonic flow around oscillating airfoils,» National Aerospace Laboratory (NLR) , Amsterdam, 1977.
- [8] J. R. v. Ommen, J. C. Schouten, M. L. v. Stappen e C. M. v. d. Bleek, «Response characteristics of probe–transducer systems for pressuremeasurements in gas–solid fluidized beds: how to prevent pitfalls indynamic pressure measurements,» *Powder Technology*, vol. 106, p. 199–218, 1999.
- [9] D. H. Zinn e D. M. Habermann, «Developements and experiences with pulsation measurements for heavy-duty gas turbines,» in *ASME Turbo Expo*, 2007.
- [10] M. A. White, M. Dhingra e J. Prasad, «Experimental analysis of a wave guide pressure measuring system,» *Journal of Engineering for Gas Turbines and Power*, vol. 132, n. 041603-1, 2010.